A&A 407, 377–384 (2003)
DOI: 10.1051/0004-6361:20030781


Astronomy & Astrophysics

# Interrelations between Vilnius and Strömgren photometric systems: The luminosity indicator *(v – X)*⋆

N. Kaltcheva[1], J. Knude[2], and V. Georgiev[3]

[1] Department of Physics & Astronomy, University of Wisconsin Oshkosh, 800 Algoma Blvd., Oshkosh, WI 54901-8644, USA
[2] Niels Bohr Institute for Astronomy, Physics and Geophysics, Juliane Maries Vej 30, 2100 Copenhagen Ø, Denmark
e-mail: indus@astro.ku.dk
[3] Department of Astronomy, University of Sofia, 5 J. Bourchier Ave., 1164 Sofia, Bulgaria
e-mail: vladimir@phys.uni-sofia.bg

Received 4 April 2003 / Accepted 18 May 2003

**Abstract.** Using the largest database of near-IR Ca II Triplet indices currently available (Cenarro et al. 2001a,b), we confirm our finding about the influence of the Ca II stellar lines on the $X$ magnitude of the Vilnius photometric system. This effect is significant for spectral sub-classes from early F until mid K. For this spectral range there is a linear relation between the $v-X$ index and the strength of the infrared Ca II Triplet, which implies that the Ca II H&K lines should influence the difference in a similar way. For the spectral interval studied, $v-X$ repeats the behavior of the Ca II Triplet with respect to gravity, temperature and metallicity. The Ca II Triplet lines are a powerful diagnostic of the stellar populations in galaxies because of their sensitivity to the main stellar atmospheric parameters. Being much easily achievable observationally and virtually reddening free, the $v-X$ index may find similar applications. $v-X$ is log $g$ sensitive but additional means are required to break the dwarf – giant duplicity. For this purpose we have studied the variation of the $v$(Strömgren)$-B$(Johnson) index with gravity, temperature and the equivalent width of the Ca II Triplet. Since $v$(Strömgren)$-B$(Johnson) have a none overlapping variation with the Ca II Triplet the dwarfs and giants may be separated and $T_{\rm eff}$ and log $g$ may be estimated. The $v$(Strömgren)$-B$(Johnson) index has furthermore the advantage that $E(v-B) \approx 0.25E(B-V)$.

**Key words.** methods: observational – techniques: photometric

## 1. Introduction

Recently we presented a number of empirically derived relationships between some Vilnius and Strömgren photometric quantities (Kaltcheva & Knude 2002; Knude & Kaltcheva 2002). In particular we investigated interrelationships between quantities related to the Balmer discontinuity, metallicity and temperature. In a comparison of all published Vilnius and Strömgren photometric data we noticed significant differences in similar indices, apparently due to small deviations of the central wavelengths and band-widths of the corresponding filters used. The deviations are most pronounced for the differently defined violet $v$ and $X$ bands. We suggested that the shift and widening of the Vilnius $X$ band introduced a metal and luminosity sensitivity not present to the same degree of the Strömgren $v$ band. After a close inspection of a number of photometric diagrams we interpreted the $v-X$ difference as caused by the Ca II H&K spectral feature. The index in fact showed a tight correlation with the hk index measuring the Ca II H&K bands, Twarog & Anthony-Twarog (1995). To check this hypothesis further we compared the $v-X$ quantity to the equivalent width (EQW hereafter) of the infrared Ca II Triplet (CaT hereafter), which were adopted from Mallik (1997). Since the Ca II H&K lines have the same upper level as the CaT lines, a correlation exists between the EQW of the H&K Ca II lines and the EQW of CaT. The collated sample contained G0-K5 stars of moderate luminosity and clearly showed a decrease of the $v-X$ difference with the increase of the EQW CaT toward the cooler spectral types. Also, the $v-X$ difference decreases with the decreasing of the log $g$ (data from Mallik 1997) and with the absolute magnitude inferred from the *Hipparcos* (ESA 1997) parallaxes, clearly indicating in this way a luminosity dependence.

Recently, Cenarro et al. (2001a,b) presented a new spectral library of the near IR-region for 706 stars with known atmospheric parameters. They defined a new set of CaT indices, specially suited to measure the CaT strength corrected for the contamination from Paschen lines. The authors also included in their database homogenized literature data for the main stellar atmospheric parameters. In the present paper we use this new database to verify and further develop the idea about the luminosity dependence of the $v-X$ photometric quantity.

Since the sample with complete $v$, $X$, CaT, parallax and astrophysical parameters is small we try to corroborate the trends discovered by studying the index $v$(Strömgren)$-B$(Johnson) in

*Send offprint requests to*: N. Kaltcheva,
e-mail: kaltchev@uwosh.edu
⋆ Based on CDS data.

some detail. We elaborate somewhat on this issue since ESA's corner stone mission GAIA, ESA (2000), may contain two photometric systems that may allow the introduction of a two band combination like the $v$(Strömgren)$-B$(Johnson) index only optimized for astrophysical purposes. Our discussion tentatively suggests that such a procedure will be feasible.

## 2. The sample

For this purpose all available Strömgren and Vilnius photometric data were collected for the stars later than F0 type and known to be non-peculiar, that were included in the Cenarro et al. (2001a,b) database. The VizieR II/157A (Photoelectric Photometry in Vilnius system) and VizieR II/215 ($uvby\beta$) Catalogs were used to collate the sample. The final sample consists of 35 stars and is presented in Table 1. There are only 4 stars in common between this new sample and the sample used before by Kaltcheva & Knude (2002). Table 1 contains the identification from the Cenarro et al. (2001a,b) database, the *Hipparcos* and HD identifications, followed by the Strömgren and Vilnius photometric data, and data about the MK classification, effective temperature, surface gravity, metallicity and the strength of the CaT, all adopted from the Cenarro et al. (2001a,b) database. Both the data about the strength of CaT, corrected for the Paschen lines (CaT*) and uncorrected for the Paschen lines (CaT) are included.

## 3. Results and discussion

### 3.1. The combined $v - X$ index

Figure 1 presents the $m_1/(b-y)$ and the $[c_1]/[m_1]$ diagrams for the new sample with the spectral and luminosity types indicated. Open circles mark main sequence (MS hereafter) stars in the spectral range F3-K3 (F3 being the earliest type in our sample, see Table 1). Open circles overlapped with filled triangles indicate the MS stars with temperature higher than 6000 K according to the data of Cenarro et al. (2001a). These are mainly F type MS stars. Open circles overlapped with open triangles indicate these MS stars with temperature lower than 5500 K (mainly K type MS stars). Open circles without an inscribed triangle cover the temperature range between 5500 and 6000 K. "+" symbols represent stars of luminosity classes IV and III, not later than K1 spectral type (7 G0-K1 stars of LC IV and III). Filled squares are used for the four stars of spectral types K3 and later, all of them of LC III. The standard line is adopted from Philip & Egret (1980) for spectral types B-G and from Olsen (1984) for O-M2 spectral range.

The first three panels in Fig. 2 present $v - X$ as a function of $v - y$, EQW CaT and EQW CaT*. It is interesting to notice that only in the $v - X$ vs. $v - y$ diagram there is a complete resolution of the effective temperature. In the $v - X$ vs. CaT* diagram it is almost as good whereas the three temperature ranges are mixed in the $v - X$ vs. CaT diagram. $v - X$ vs. CaT* diagram also shows a complete resolution of the luminosity class. This might indicate that proper photometric indices can help break the degeneracies of the parameters determined from the CaT spectroscopy.

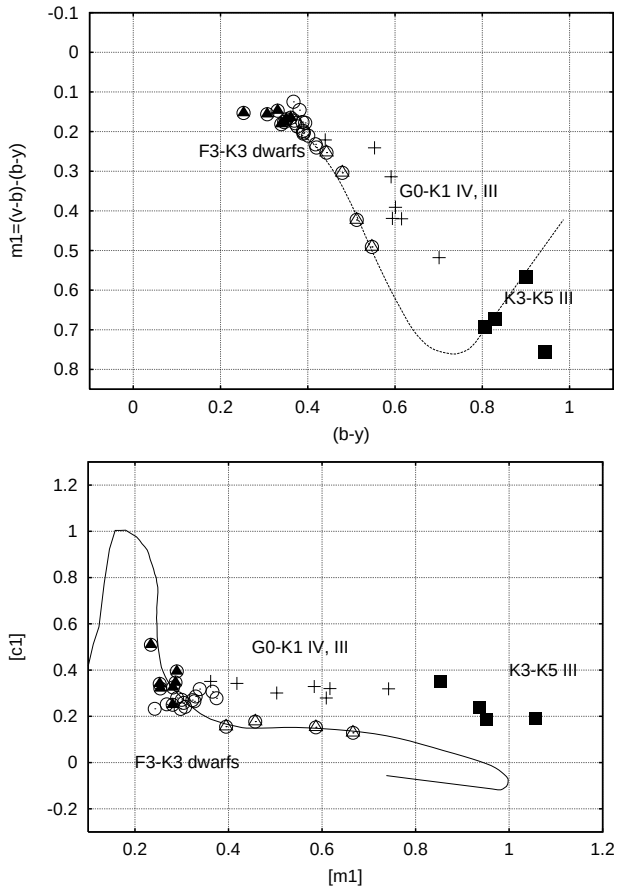


**Fig. 1.** The $m_1/(b-y)$ and the $[c_1]/[m_1]$ diagrams for the sample. For MS stars open circles are used. Filled and open triangles overlap the open circles to indicate MS stars with temperature higher than 6000 K and lower than 5500 K respectively (please see Fig. 3, first panel). "+" symbols are used for stars of luminosity classes IV and III, of spectral type K2 and earlier. Filled squares are used for the K3-K5 III stars.

In general a tight correlation exists between $v - X$ and CaT or CaT* quantities and the standard deviations and coefficients of the linear fitting are given in Table 2. The dependence of CaT* shows a slightly better correlation. Please, note that the photometry of these stars comes from different sources and this could increase the scatter of the relationships. Just for comparison, the fourth panel presents the $v - X$ vs. EQW CaT relationship for the old sample (Kaltcheva & Knude 2002), which shows a similar behavior but the $v - X$ correlation with Cenarro's et al. data is tighter than with Mallik's CaT data. Apart from one star the MS relation of the Mallik sample is otherwise comparable to the relation for the new sample.

In the literature, the infrared triplet lines of ionized calcium have been widely analysed to investigate their dependence on stellar parameters like luminosity, temperature and metallicity. The results point out a complex behavior of the EQW CaT over the spectral and luminosity range. Jones et al. (1984) observed the CaT in 62 stars (early B to mid M), including a wide range of surface gravity and metallicity. Their data revealed the existence of an almost single valued relation between the EQW CaT and log $g$ for F to the mid M range.

**Table 1.** The new sample: identifications from the Cenarro et al. (2001a,b) database, Hipparcos and HD catalogues, followed by the Strömgren and Vilnius photometric data, and data about the MK classification, effective temperature, surface gravity, metallicity and the strength of the CaT corrected for the Paschen lines (CaT*) and uncorrected for the Paschen lines (CaT).

| CNo | HIP | HD | $V$ | $b-y$ | $m_1$ | $c_1$ | $U-P$ | $P-X$ | $X-Y$ | $Y-Z$ | $Z-V$ | $V-S$ | MK | $T_{\rm eff}$ | log $g$ | [Fe/H] | CaT* | CaT |
|---|---|---|---|---|---|---|---|---|---|---|---|---|---|---|---|---|---|---|
| **F3-K3** | | | | | | | | | | | | | | | | | | |
| **dwarfs** | | | | | | | | | | | | | | | | | | |
| 505 | 88175 | 164259 | 4.62 | 0.253 | 0.153 | 0.560 | 0.51 | 0.62 | 0.59 | 0.28 | 0.14 | 0.39 | F3V | 6737 | 4.000 | –0.02 | 5.013 | 7.525 |
| 9 | 60304 | 107611 | 8.51 | 0.307 | 0.156 | 0.382 | 0.46 | 0.55 | 0.65 | 0.30 | 0.18 | 0.47 | F6V | 6402 | 4.270 | –0.05 | 5.306 | 6.722 |
| 643 | 112447 | 215648 | 4.20 | 0.331 | 0.147 | 0.407 | 0.50 | 0.58 | 0.66 | 0.31 | 0.18 | 0.49 | F7V | 6169 | 4.020 | –0.30 | 4.886 | 6.331 |
| 662 | 114924 | 219623 | 5.58 | 0.351 | 0.169 | 0.395 | 0.46 | 0.58 | 0.74 | 0.33 | 0.20 | 0.49 | F7V | 6155 | 4.170 | –0.04 | 6.366 | 7.378 |
| 184 | 7513 | 9826 | 4.10 | 0.346 | 0.176 | 0.415 | 0.48 | 0.62 | 0.71 | 0.31 | 0.22 | 0.48 | F8V | 6135 | 4.080 | 0.11 | 6.358 | 8.335 |
| 650 | 113896 | 217877 | 6.68 | 0.369 | 0.172 | 0.353 | 0.46 | 0.59 | 0.75 | 0.33 | 0.20 | 0.51 | F8V | 5866 | 4.020 | –0.19 | 6.070 | 6.874 |
| 11 | 60406 | 107793 | 9.10 | 0.361 | 0.165 | 0.322 | 0.42 | 0.54 | 0.70 | 0.32 | 0.17 | 0.58 | F8V | 6032 | 4.340 | –0.05 | 4.814 | 6.053 |
| 471 | 80837 | 148816 | 7.27 | 0.367 | 0.125 | 0.306 | 0.45 | 0.52 | 0.65 | 0.36 | 0.19 | – | F8V | 5831 | 4.220 | –0.73 | 5.073 | 5.834 |
| 363 | 60098 | 107213 | 6.38 | 0.339 | 0.181 | 0.462 | 0.49 | 0.65 | 0.73 | 0.31 | 0.20 | 0.50 | F8Vs | 6302 | 4.010 | 0.29 | 6.711 | 8.267 |
| 454 | 77760 | 142373 | 4.60 | 0.381 | 0.146 | 0.328 | 0.47 | 0.56 | 0.73 | 0.32 | 0.19 | 0.53 | F9V | 5821 | 4.130 | –0.41 | 5.680 | 6.489 |
| 8 | 60293 | 107583 | 9.31 | 0.376 | 0.187 | 0.316 | 0.46 | 0.59 | 0.78 | 0.32 | 0.22 | 0.55 | G01V | 5918 | 4.380 | –0.05 | 5.732 | 6.810 |
| 5 | 60097 | 107214 | 9.02 | 0.371 | 0.179 | 0.306 | 0.40 | 0.57 | 0.77 | 0.32 | 0.19 | 0.56 | G0V | 5918 | 4.300 | –0.05 | 5.934 | 6.844 |
| 160 | 1499 | 1461 | 6.47 | 0.420 | 0.240 | 0.362 | 0.49 | 0.70 | 0.90 | 0.37 | 0.21 | 0.55 | G0V | 5816 | 4.300 | 0.20 | 7.193 | 8.004 |
| 347 | 53721 | 95128 | 5.03 | 0.391 | 0.202 | 0.343 | 0.44 | 0.62 | 0.82 | 0.34 | 0.21 | 0.54 | G0V | 5834 | 4.340 | 0.04 | 6.732 | 7.527 |
| 243 | 24813 | 34411 | 4.69 | 0.390 | 0.205 | 0.364 | 0.46 | 0.65 | 0.83 | 0.34 | 0.22 | 0.56 | G0V | 5835 | 4.170 | 0.06 | 6.715 | 7.741 |
| 333 | 49081 | 86728 | 5.37 | 0.418 | 0.232 | 0.390 | 0.45 | 0.72 | 0.87 | 0.33 | 0.23 | 0.58 | G1V | 5742 | 4.210 | 0.13 | 7.395 | 8.049 |
| 604 | 103682 | 199960 | 6.21 | 0.401 | 0.210 | 0.398 | 0.48 | 0.67 | 0.86 | 0.32 | 0.23 | 0.55 | G1V | 5773 | 4.190 | 0.18 | 7.250 | 8.488 |
| 185 | 7918 | 10307 | 4.96 | 0.389 | 0.198 | 0.348 | 0.46 | 0.63 | 0.82 | 0.33 | 0.21 | 0.55 | G2V | 5847 | 4.280 | 0.02 | 6.081 | 6.081 |
| 458 | 78459 | 143761 | 5.39 | 0.394 | 0.178 | 0.337 | 0.45 | 0.62 | 0.78 | 0.34 | 0.21 | 0.53 | G2V | 5762 | 4.230 | –0.20 | 6.162 | 7.086 |
| 168 | 3559 | 4307 | 6.15 | 0.388 | 0.176 | 0.349 | 0.46 | 0.61 | 0.76 | 0.36 | 0.19 | 0.55 | G2V | 5742 | 4.070 | –0.25 | 5.742 | 6.638 |
| 188 | 8102 | 10700 | 3.49 | 0.443 | 0.253 | 0.244 | 0.43 | 0.68 | 0.90 | 0.33 | 0.25 | 0.61 | G8V | 5264 | 4.360 | –0.50 | 6.286 | 6.697 |
| 426 | 73005 | 132142 | 7.77 | 0.479 | 0.304 | 0.273 | 0.42 | 0.77 | 1.04 | 0.34 | 0.28 | 0.65 | K1V | 5108 | 4.500 | –0.55 | 6.726 | 7.154 |
| 170 | 3765 | 4628 | 5.74 | 0.512 | 0.423 | 0.255 | 0.40 | 0.91 | 1.21 | 0.32 | 0.34 | 0.73 | K2V | 4960 | 4.600 | –0.29 | 6.535 | 7.164 |
| 460 | 78913 | 144872 | 8.58 | 0.547 | 0.491 | 0.238 | 0.41 | 0.93 | 1.30 | 0.30 | 0.40 | 0.77 | K3V | 4739 | 4.650 | –0.31 | 6.229 | 6.892 |
| **G0-K1** | | | | | | | | | | | | | | | | | | |
| **LC IV, III** | | | | | | | | | | | | | | | | | | |
| 180 | 5454 | 6903 | 5.57 | 0.440 | 0.221 | 0.439 | 0.59 | 0.67 | 0.88 | 0.39 | 0.23 | 0.60 | G0III | 5570 | 2.900 | – | 7.651 | 8.859 |
| 165 | 3031 | 3546 | 4.34 | 0.553 | 0.241 | 0.453 | 0.59 | 0.78 | 1.05 | 0.43 | 0.25 | 0.68 | G5III... | 4942 | 2.730 | –0.66 | 6.660 | 7.337 |
| 636 | 110003 | 211391 | 4.17 | 0.594 | 0.419 | 0.398 | 0.58 | 0.95 | 1.27 | 0.48 | 0.29 | 0.71 | G8III-IV | 4943 | 2.700 | 0.08 | 8.048 | 8.683 |
| 250 | 26366 | 37160 | 4.09 | 0.591 | 0.314 | 0.419 | 0.58 | 0.86 | 1.17 | 0.44 | 0.30 | 0.75 | G8III-IV | 4668 | 2.460 | –0.50 | 8.258 | 8.409 |
| 461 | 79137 | 145148 | 5.93 | 0.601 | 0.391 | 0.449 | 0.52 | 1.01 | 1.28 | 0.40 | 0.34 | 0.75 | K0IV | 4849 | 3.450 | 0.10 | 7.466 | 7.799 |
| 453 | 77655 | 142091 | 4.79 | 0.615 | 0.420 | 0.443 | 0.57 | 1.04 | 1.29 | 0.42 | 0.32 | 0.71 | K0III-IV | 4796 | 3.220 | 0.00 | 7.655 | 8.214 |
| 456 | 78132 | 142980 | 5.54 | 0.701 | 0.518 | 0.459 | 0.58 | 1.14 | 1.48 | 0.45 | 0.39 | 0.80 | K1IV | 4549 | 2.740 | 0.11 | 7.850 | 8.185 |
| **K3-K5** | | | | | | | | | | | | | | | | | | |
| **LC III** | | | | | | | | | | | | | | | | | | |
| 186 | 7884 | 10380 | 4.45 | 0.830 | 0.672 | 0.404 | 0.71 | 1.34 | 1.83 | 0.54 | 0.45 | 0.94 | K3III | 4057 | 1.430 | –0.25 | 8.542 | 9.093 |
| 574 | 97635 | 188056 | 5.03 | 0.806 | 0.693 | 0.346 | 0.64 | 1.36 | 1.74 | 0.50 | 0.45 | 0.87 | K3IIIvar | 4244 | 2.010 | 0.17 | 8.721 | 9.456 |
| 552 | 94929 | 180928 | 6.09 | 0.900 | 0.566 | 0.529 | 0.78 | 1.32 | 1.79 | 0.54 | 0.49 | 0.99 | K4III | 4000 | 1.300 | –0.38 | 8.671 | 8.816 |
| 437 | 74901 | 136028 | 5.88 | 0.943 | 0.755 | 0.378 | 0.78 | 1.37 | 2.00 | 0.59 | 0.49 | 1.04 | K5III | 3995 | 1.900 | 0.19 | 10.093 | 10.454 |

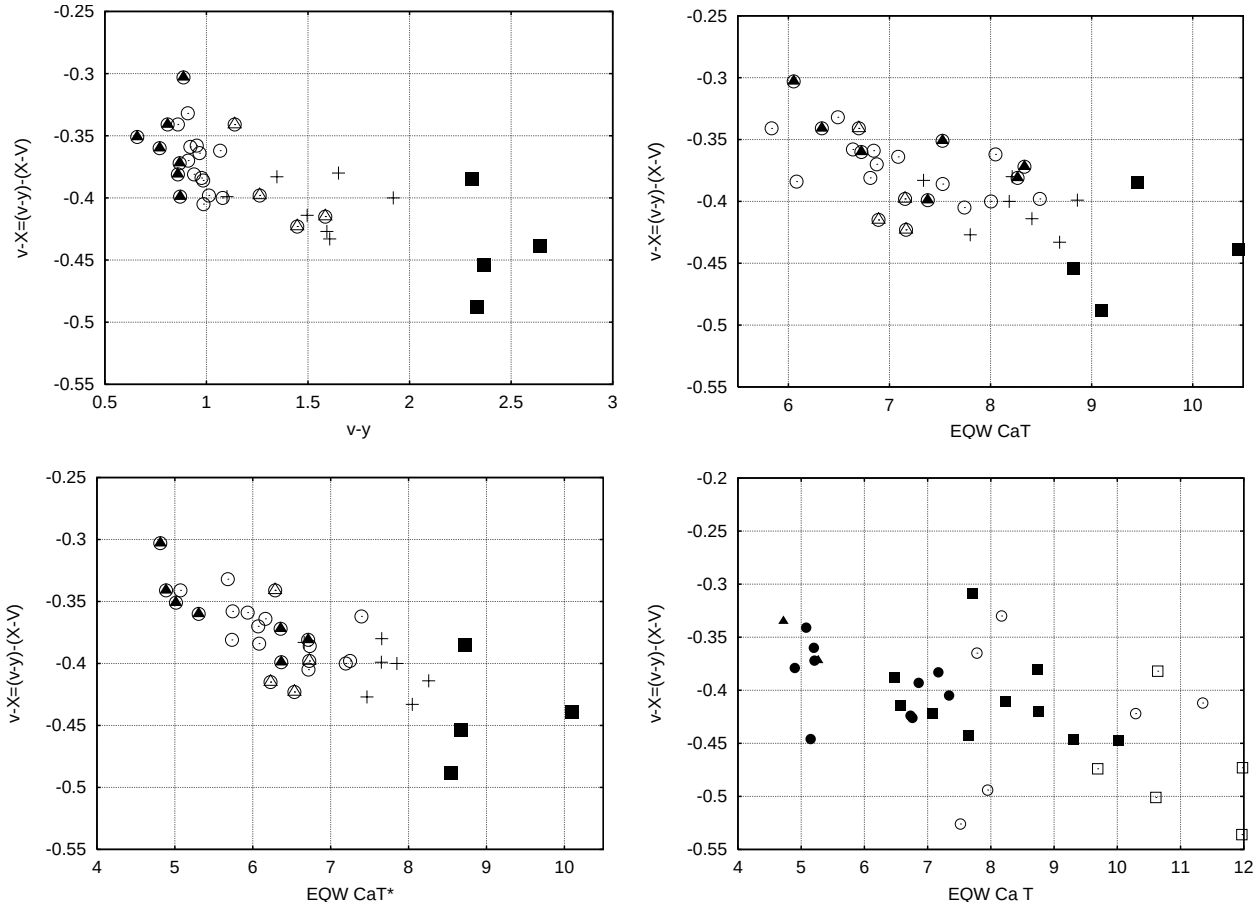


**Fig. 2.** First three panels: $v - X$ as a function of $v - y = m_1 + 2(b - y)$, EQW CaT and EQW CaT*. Apart from being metal dependent $m_1$ is also temperature sensitive. $b - y$ is of course also $T_{\rm eff}$ dependent implying that the $v - X$ vs. $v - y$ variation could be due to the temperature variation that is noticed from the spectral type coding of the plotting symbols. The symbols at the first three panels are the same as in Fig. 1. Last panel (to the lower right): the comparison of $v-X$ to EQW CaT based on our old sample with CaT data from Mallik (1997): open and filled symbols indicate stars more and equal and less luminous of LCIII respectively, circles and squares indicate G and K type stars respectively; filled triangles indicate the two F-type MS stars included in the previous sample.

Alloin & Bica (1989) concluded that CaT has a significant dependence on metallicity. Diaz et al. (1989) and Zhou (1991) suggested that the CaT strength depends both upon gravity and metallicity. Jones et al. (1984) have also tested theoretically the sensitivity of the CaT to the surface gravity, effective temperature and calcium abundance. For giants and supergiants they noticed a rapid decrease of the EQW CaT with increasing log $g$ whereas the relation is flatter for dwarfs. Erdelyi-Mendes & Barbuy (1991) noted that the metallicity dependence of CaT becomes evident only when a large parameter space is covered. In general the theoretical analysis shows that the strong underlying relationship between the EQW CaT and log $g$ is modified by the calcium abundance and perhaps $T_{\rm eff}$ and giants and dwarfs respond differently to the change in metallicity. The more recent study by Mallik (1994, 1997) revealed a strong (non-linear) dependence on luminosity, much stronger for metal rich stars than for the metal poor ones and a milder dependence on metallicity, although much more conspicuous in supergiants than in dwarfs. The complex behavior of the CaT strength as a function of the three main atmospheric parameters is again emphasized by Cenarro et al. (2002). With the good correlation between $v - X$ and EQW CaT* (Fig. 2) we may expect to calibrate this index in a similar way as the infrared triplet may be calibrated.

Figure 3 shows the dependencies between different physical parameters plotted for the stars of our sample. The EQW CaT*, $T_{\rm eff}$, log $g$, [Fe/H] are adopted from the Cenarro et al. (2001a,b) database and the absolute visual magnitudes $M_V$HIP are inferred from *Hipparcos*. There is a general $T_{\rm eff}$ decrease with EQW CaT* but $T_{\rm eff}$ can not be determined with EQW CaT* in the range from ~6 to ~8. In particular we notice that the stars with temperatures in the range from 5500 to 6000 K (open circles without inscribed triangle) show a considerable EQW CaT* range. This degeneracy might however be broken by replacing CaT* with $v - X$, see upper left of Fig. 4. In general, our Fig. 3 is similar to the plots presented by Jones et al. (1984) and Cenarro et al. (2002). No clear metallicity dependence of the CaT* index can be noticed for the whole sample (see CaT* vs. [Fe/H] plot) and dwarfs and giants are clearly separated on all graphs. The overall impression is that stars more luminous according to the $m_1$ vs. $b - y$ diagram (and respectively to their luminosity classifications)

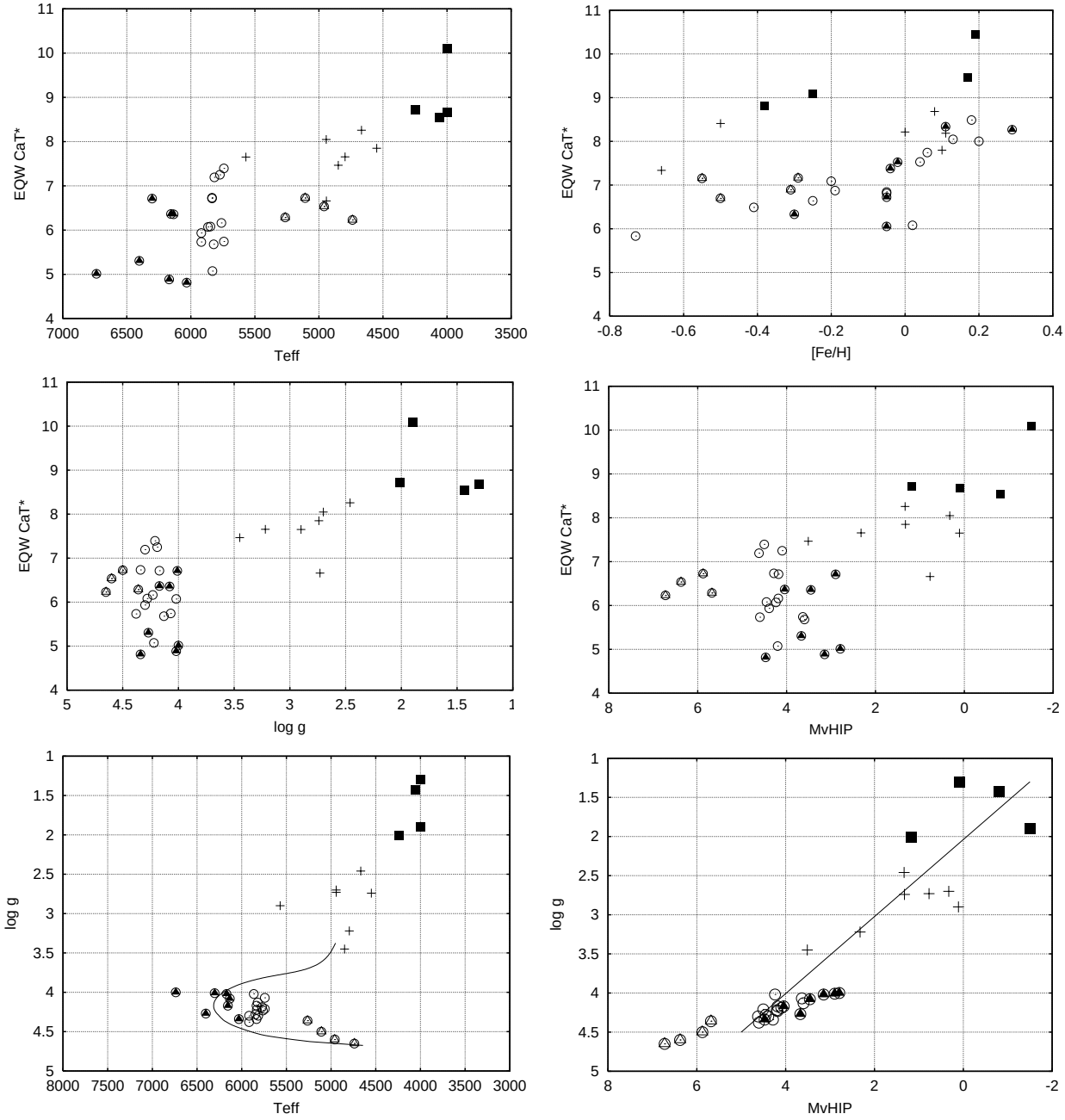


**Fig. 3.** Dependencies between EQW CaT*, $T_{\rm eff}$, log $g$, [Fe/H] and $M_V$HIP. The symbols are the same as in Fig. 1 The curve in bottom left frame is an isochrone with age 6 Gyr and [Fe/H] = −0.25 from Vandenberg (1985).

have larger CaT* index and smaller log $g$ and are intrinsically brighter according to their *Hipparcos* absolute magnitudes as well. As noted above, for luminosity class V the EQW CaT* only slightly changes over the 6800–5800 K temperature range (although the different spectral types are clearly distinguishable) in comparison to the overall trend from dwarfs to giants. Likewise, in the log $g$ vs. $T_{\rm eff}$ diagram the luminosity class V stars have similar log $g$ values over a temperature range of some 1000 K. The luminosity dependence of the CaT* index can be clearly followed on CaT* vs. log $g$ and vs. $M_V$HIP plots. In the log $g$ vs. $M_V$HIP diagram the MS stars with $T_{\rm eff}$ less than about 5500 K might form a separate group, also noticeable in the $v - X$ vs. $M_V$HIP diagram (Fig. 4). The larger scatter on the CaT* vs. $M_V$HIP plot in comparison to log $g$ vs. $M_V$HIP plot reflects probably a mild temperature dependence of CaT*.

**Table 2.** The coefficients of the linear fittings of $(v - y) - (X - V) = A$ CaT (or CaT*) $+B$.

| | $A$ | $B$ | st.dev. |
|---|---|---|---|
| CaT | −0.026 ± 0.005 | −0.182 ± 0.037 | 0.021 |
| CaT* | −0.024 ± 0.004 | −0.219 ± 0.024 | 0.019 |

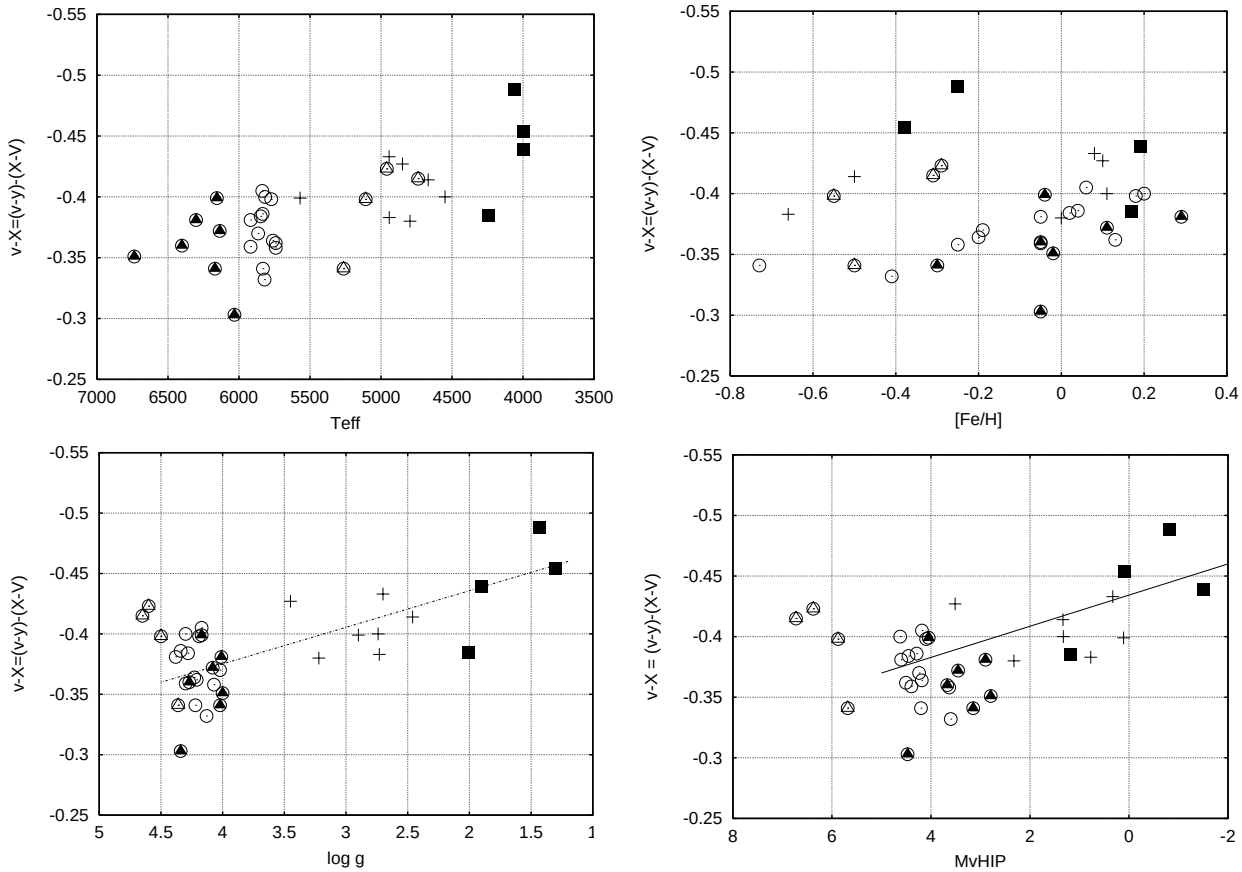


**Fig. 4.** Dependencies between $v - X$ and $T_{\rm eff}$, log $g$, [Fe/H] and $M_V$HIP. The symbols are the same as in Fig. 1.

Figure 4 presents the dependencies between $v - X$ and the stellar parameters $T_{\rm eff}$, log $g$, [Fe/H] and $M_V$HIP. For the F-K spectral range the $v - X$ index repeats the behavior of CaT with respect to the gravity, temperature and metallicity, seen in Fig. 3. Again, the trend seen is likely to be due to the influence of the luminosity change from early F dwarfs to mid K subgiants and giants on the $X$ pass-band and correlates with the absolute magnitude inferred from *Hipparcos*. No dependence of the metallicity is noticed.

In the lower left panel of Fig. 4 we may just see an indication of that the slope of $v - X$ vs. log $g$ changes sign at log $g \approx 4.0$–$4.5$ showing that stars from the MS and evolved stars may have a different log $g$ dependence on $v - X$. MS stars may have $\partial \log g/\partial(v - X) < 0$ whereas the evolved stars have $\partial \log g/\partial(v - X) > 0$. This issue must of course be solved if a $v - X$ vs. log $g$ relation is to be established. The reality of the change of sign of the derivatives is corroborated of our discussion of the $v - B$ index in the next section. As expected a similar behavior is seen in the $M_V$HIP vs. $v - X$ diagram. Admittedly the CaT* sample contains too few stars for a firm conclusion but fortunately is the $v$, $B$, CaT* sample discussed in the next section somewhat larger, see the lower two panels of Fig. 5.

The lower left panel of Fig. 4 is the equivalent of the HR diagram. The turn off is located at $(v - X, \log g) \approx (-0.33, 4.2)$. The sample is seen to include no main sequence stars hotter than the turn off as it should not according to the classification given in Table 1.

### 3.2. Comparisons between Johnson and Strömgren quantities: v – B

To give a more clear insight on the relations between $v - X$ quantity and the main stellar parameters, we present in Fig. 5 a comparison between $v - B$ quantity and EQW CaT*, log $g$ and $T_{\rm eff}$. $v - B$ is obtained as a difference between $v - y$ and $B - V$ and corresponds to $v - X$ in the combination of the Strömgren and Johnson systems. The sample in Fig. 5 is the largest sample possible that presently can be selected with published Johnson and Strömgren photometry and CaT measurements. The upper left panel in Fig. 5 gives an impression about the spectral and luminosity content of the sample, which consists mainly of A-K V-III stars. A subsample of all stars with Vilnius and Strömgren photometry and CaT measurements *and* Johnson photometry shows same general behavior and is not presented here.

The upper right panel of Fig. 5 may be compared to the upper right of Fig. 2. The kink noticed in Fig. 5 is apparently absent in Fig. 2. In Fig. 5 LC V and LC III seem to be nicely separated, perhaps even better than the +'s and ∘'s indicate because according to the giant – main sequence separation in the $[c_1]$ vs. $[m_1]$ diagram three dwarfs ($m_1 = 0.7$, $c_1 = 0.3$) rightly should be classified as giants thus making the luminosity separation of the $v - B$ vs. CaT* diagram clearer. The bottom left panel shows the $v - B$ vs. [Fe/H] variation for the $v$, $B$ sample. Again, no dependence of the metallicity is noticed, which is a

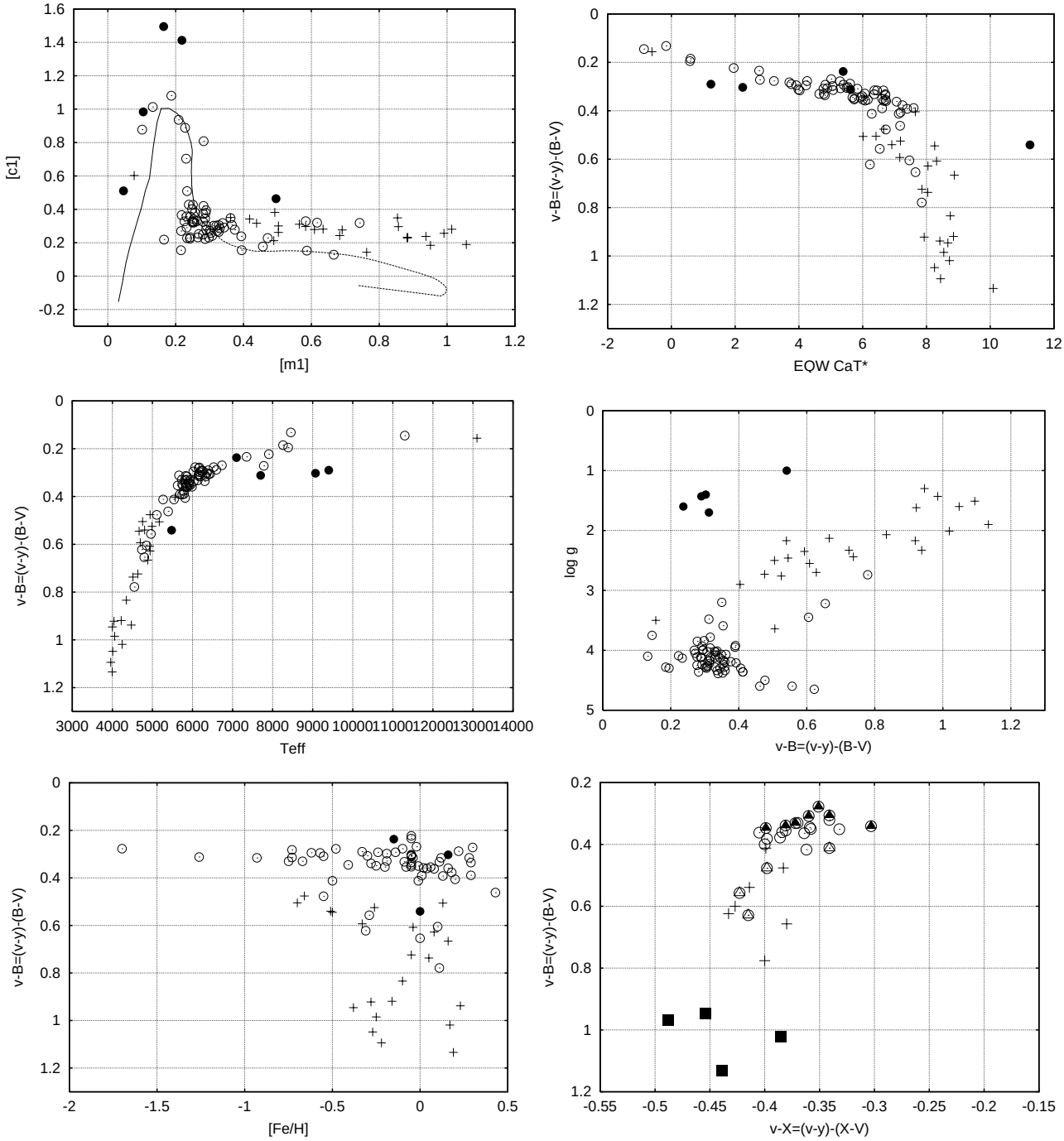


**Fig. 5.** The $[c_1]/[m_1]$ diagram (standard line is the same as in Fig. 1) and dependencies between $v - B$ and and EQW CaT, $T_{\rm eff}$, log $g$ and [Fe/H] for the sample with Strömgren and Johnson photometry and CaT measurements available. Open circles represent stars of LC IV and V. This sub-sample contains spectral types in the A0-K3 range. Crosses are used for LC IV-III and III. This sub-sample contains stars of spectral types G0-K5 (and one B7 star). Filled circles are used for LC Ia and Ib – five such stars in the A0-G0 spectral range are included in our sample. Bottom right: $v - B$ vs. $v - X$; the symbols for this plot are the same as in Fig. 1.

little unexpected since the $v$ band does contain metal lines used in the Strömgren system to measure metallicity. The bottom right panel displays the $v - B$ vs. $v - X$ variation for the small Vilnius, Strömgren, CaT* sample. There is a rough linear dependence but with a huge scatter. Even in this diagram we note that the temperature of the main sequence stars separate quite well.

One can notice the different behavior of $v - X$ and $v - B$ with respects to CaT and the main stellar parameters. $v - B$ vs. log $g$ plot shows a clear separation due to luminosity, but in the $v - B$ vs. CaT plot we see overlap for stars of different LC and same spectral type. Such a behavior is absent on the $v - X$ vs. CaT* plot. This implies that $v - X$ is more temperature free than $v - B$. $v - X$ vs. CaT* relation is presented by

a single linear sequence over the luminosity range, and can be calibrated in terms of Ca II T for F-K types, as indicated both by the sample previously used (Kaltcheva & Knude 2002) and the new sample. One must however considerer the LC overlap in the light of the recent result by Gray et al. (2001). They find strong evidence that the luminosity type is not a particularly good indicator of the absolute magnitude in the spectral type range from A5 to about mid K. Microturbulence seems equally important for the luminosity classification.

Indices like the $v - B$ index may prove important in the context of ESA's GAIA mission in providing "reddening free" indices correlating well with astrophysical parameters in a simple way, may be not resulting in the most accurate parameter but giving a reliable range that may be used in a preclassification to be fed into a neural network (or some other classification procedure). The medium-wide band combination will be particularly useful for GAIA since it may have both a wide band system for chromatic correction of the astrometry and a medium band system for astrophysical properties. If these systems are designed with a medium band located on some astrophysical interesting features (or spectral region) and a wide band with an identical central wavelength the reddening effect of the interstellar medium may be avoided to some extent. A rough estimate shows that $E(v-B) \approx 0.25 \times E(B-V) \approx 0.33 \times E(b-y)$. Figure 5 may accordingly give a rather good $T_{\rm eff}$ estimate even without the proper reddening correction. For a star with $A_V = 1$ mag the neglected reddening correction will introduce an uncertainty in $v - B$ less than 0.1 and according to the slope of $T_{\rm eff}$ vs. $v - B$ in Fig. 5 this will introduce a $T_{\rm eff}$ uncertainty ~200 K. If $T_{\rm eff}$ was based on $b-y$ for the same star with $A_V = 1$ mag and the photometry was not dereddened the $T_{\rm eff}$ uncertainty would exceed 1000 K, for a sharp $b - y - T_{\rm eff}$ relation see e.g. Fig. 3 of Gray et al. op. cit.

As seen in the center – right panel of Fig. 5 $v - B$ shows a variation with $\log g$ as $v - X$ did, only more pronounced due to the larger sample and possibly due to the better scale of $v - B$: $\partial \log g/\partial(v-B) > 0$ for dwarfs and $\partial \log g/\partial(v-B) < 0$ for giants. Due to the larger v, $B$ sample these trends are more clearly displayed in Fig. 5 than they were in Fig. 4. The $\log g$ vs. $v - B$ diagram is again a presentation of the HR diagram and in this sample a few main sequence stars hotter than the turn off are included and the diagram shows the super giants to follow the giant sequence. The $\log g$ vs. $v - B$ diagram in fact looks very similar to Fig. 6 of Cenarro et al. (2002). If a giant – main sequence distinction can be provided by other means an index like $v - B$ could be used as a $\log g$ estimator or as an absolute magnitude estimator like $v - X$ in the lower right panel of Fig. 4. This means that together with the measured parallax the extinction can be provided. The dwarf – giant separation thus proves rather important. This separation is possible from the $v - B$ vs. EQW CaT* diagram in the upper right panel of Fig. 5. The radial velocity measurements of GAIA is proposed to make use of the CaT and might possibly also provide the equivalent width of the triplet in addition to the radial velocity (ESA 2000, p. 134). When the evolutionary status has been ascertained $v - B$ may provide the $\log g$ estimate.

## 4. Conclusion

Since the violet spectral region is rich in lines, a $v - X$ photometric index could hold itself a valuable information. For the F-K spectral classes, we found a strong correlation between $v - X$ and the strength of the near-IR CaT. Since the strength of the CaII H&K stellar lines behaves similarly to that of the CaT, the $v - X$ index may be considered as a measure of the strength of the CaII H&K spectral feature. In general, the $v - X$ photometric quantity behaves similarly to the CaT index with respect to the physical stellar parameters. The further interpretation of the $v - X$ index as a temperature, luminosity or metallicity indicator depends on the interpretation of the relation of the CaT strength to these parameters. Based on two different samples of F-K stars, the $v - X$ index appears to be a good luminosity indicator, which is virtually reddening free because of the closeness of the $v$ and $X$ central wave lengths.

The CaT feature is an useful discriminant for the dwarf/giant ratio of the light-dominant galactic stellar population, since most of the light from galaxies is thought to come from G and K stars. Similarly, the $v-X$ photometric index could find an application in the investigation of the stellar population of distant galaxies – both in integral light when studying distant galaxies, or via surface photometry when studying the distribution of different luminosity types of face-on galaxies. The $v - X$ index is easy to be obtained photometrically. Because it is reddening-free, it can be used for large samples of stars, and applied to regions with non-uniform absorption.

*Acknowledgements.* This research has made use of the Simbad database, operated at CDS, Strasbourg, France.

## References

Alloin, D., & Bica, E. 1989, A&A, 217, 57
Cenarro, A. J., Cardiel, N., Gorgas, J., et al. 2001a, MNRAS, 326, 959
Cenarro, A. J., Gorgas, J., Cardiel, N., et al. 2001b, MNRAS, 326, 981
Cenarro, A. J., Gorgas, J., Cardiel, N., Vazdekis, A., & Peletier, R. F. 2002, MNRAS, 329, 863
Diaz, A. I., Terlevich, E., & Terlevich, R. 1989, MNRAS, 239, 325
Erdelyi-Mendes, M., & Barbuy, B. 1991, A&A, 241, 176
ESA 1997, The Hipparcos and Tycho Catalogues, ESA SP-1200, vol. 1–17
ESA 2000, GAIA, Composition, Formation and Evolution of the Galaxy, Concept and Study Report, ESA-SCI(2000)4
Gray, R. O., Graham, P. W., & Hoyt, S. R. 2001, AJ, 121, 2159
Jones, J. E., Alloin, D. M., & Jones, B. J. T. 1984, ApJ, 283, 457
Kaltcheva, N., & Knude, J. 2002, A&A, 385, 1107
Knude, J., & Kaltcheva, N. 2002, Census of the Galaxy: Challenges for Photometry and Spectrometry with GAIA, European Meet., July 2001, Vilnius, Lithuania, ed. V. Vansevicius, A. Kucinskas, & J. Sudziusin, Ap&SS, 280, 67
Mallik, S. V. 1994, A&AS, 103, 279
Mallik, S. V. 1997, A&AS, 124, 359
Olsen, E. H. 1984, A&AS, 57, 443
Philip, A. D., & Egret, D. 1980, A&AS, 40, 199
Twarog, B. A., & Anthony-Twarog, B. J. 1995, AJ, 109, 2828
Vandenberg, D. 1985, ApJS, 58, 711
Zhou, X. 1991, A&A, 248, 367